

# RSC Advances



This is an *Accepted Manuscript*, which has been through the Royal Society of Chemistry peer review process and has been accepted for publication.

*Accepted Manuscripts* are published online shortly after acceptance, before technical editing, formatting and proof reading. Using this free service, authors can make their results available to the community, in citable form, before we publish the edited article. This *Accepted Manuscript* will be replaced by the edited, formatted and paginated article as soon as this is available.

You can find more information about *Accepted Manuscripts* in the [Information for Authors](#).

Please note that technical editing may introduce minor changes to the text and/or graphics, which may alter content. The journal's standard [Terms & Conditions](#) and the [Ethical guidelines](#) still apply. In no event shall the Royal Society of Chemistry be held responsible for any errors or omissions in this *Accepted Manuscript* or any consequences arising from the use of any information it contains.

## COMMUNICATION

## 3D printed modules for integrated microfluidic devices

Cite this: DOI: 10.1039/x0xx00000x

Kyoung G. Lee<sup>a</sup>, Kyun Joo Park<sup>b</sup>, Seunghwan Seok<sup>b</sup>, Sujeong Shin<sup>a</sup>, Do Hyun Kim<sup>b</sup>, Jung Youn Park<sup>c</sup>, Yun Seok Heo<sup>d</sup>, Seok Jae Lee<sup>a,\*</sup> and Tae Jae Lee<sup>a,\*</sup>

Received 00th January 2014,  
Accepted 00th January 2014

DOI: 10.1039/x0xx00000x

[www.rsc.org/](http://www.rsc.org/)

**Ever increasing demand in integrated microfluidic devices, the advanced fabrication method requires for expanding their capability in research areas. We propose three-dimensional (3D) printing technique for producing functional modules and their assembly into integrated microfluidic device for non-expert users.**

### Introduction

The fast and cost-effective way to produce modulated microfluidic component for non-expert users has brought great interests in microfluidic-based researches including chemical, biological, and medical applications.<sup>1–3</sup> So far, B. Kintses and co-workers propose a concept to make individual microfluidic modules into integrated devices for potential diagnostics and drug screening system.<sup>4</sup> S. M. Langelier *et al.*, also develop a similar concept to build customized microfluidic systems using PDMS-based components.<sup>5</sup> Based on previous works from those pioneers, the combination of soft lithography and polydimethylsiloxane (PDMS) are common and popular ways to make microfluidic modules. Although their great efforts and advancement, conventional lithography requires complicated processes and expensive equipment and facility to construct customized microfluidic devices. Moreover, mechanical instability in the interconnection of PDMS-based components becomes a bottle-neck to operate the integrated device under high pressure.

Recently, 3D printing technique has been popular to scientists and engineers for making prototype,<sup>6</sup> reactionware,<sup>7,8</sup> tissue and organ engineering.<sup>9,10</sup> Because of its simplicity, cost-effectiveness, accuracy, and potential productivity, 3D printers allow to transfer complicated 3D designs into functional micro-to bulk-scale structure. Thus, multiple layer-by-layer depositions of UV curable polymers create multidimensional

objects. Despite of their potential, it is rarely employed in microfluidic research areas so far.<sup>11,12</sup>

To meet such challenges, herein, we propose an advanced fabrication and assembly method for modulated microfluidic devices. The general microfluidic components were made and assembled with each other into functional devices. The combination of rubber O-ring and metal pins improved module connectivity. Furthermore, non-expert users can easily access and utilize them into desirable integrated microfluidic devices without any facility limitations. We were also demonstrated and confirmed the biosensing applicability of the device using alpha-fetoprotein (AFP) biomarker detection.

### Result and Discussion

#### Block design

To construct a multifunctional microfluidic device, the operating blocks were carefully selected from well-known standard component as shown in Fig. 1a and Table S1. Each module has different functionality and acts as basic building units to construct functional microfluidic device. The concave and convex cone-shaped features were incorporated on the each side wall as mechanical alignment. The outer dimension of module is  $30 \times 30 \times 5 \text{ mm}^3$  for width, height, and length, respectively. The detailed dimensions of each module were presented in Table S1.

Another unique design of those components is each element can be assembled in all X, Y, and Z-axis depends on the experimental purpose of the devices. On the upper face of each module corner have two holes to connect with each other using horseshoe-shaped pins to enhance connectivity as shown in Fig. 1b. At the end of the channels, shallow circles were also located

## COMMUNICATION

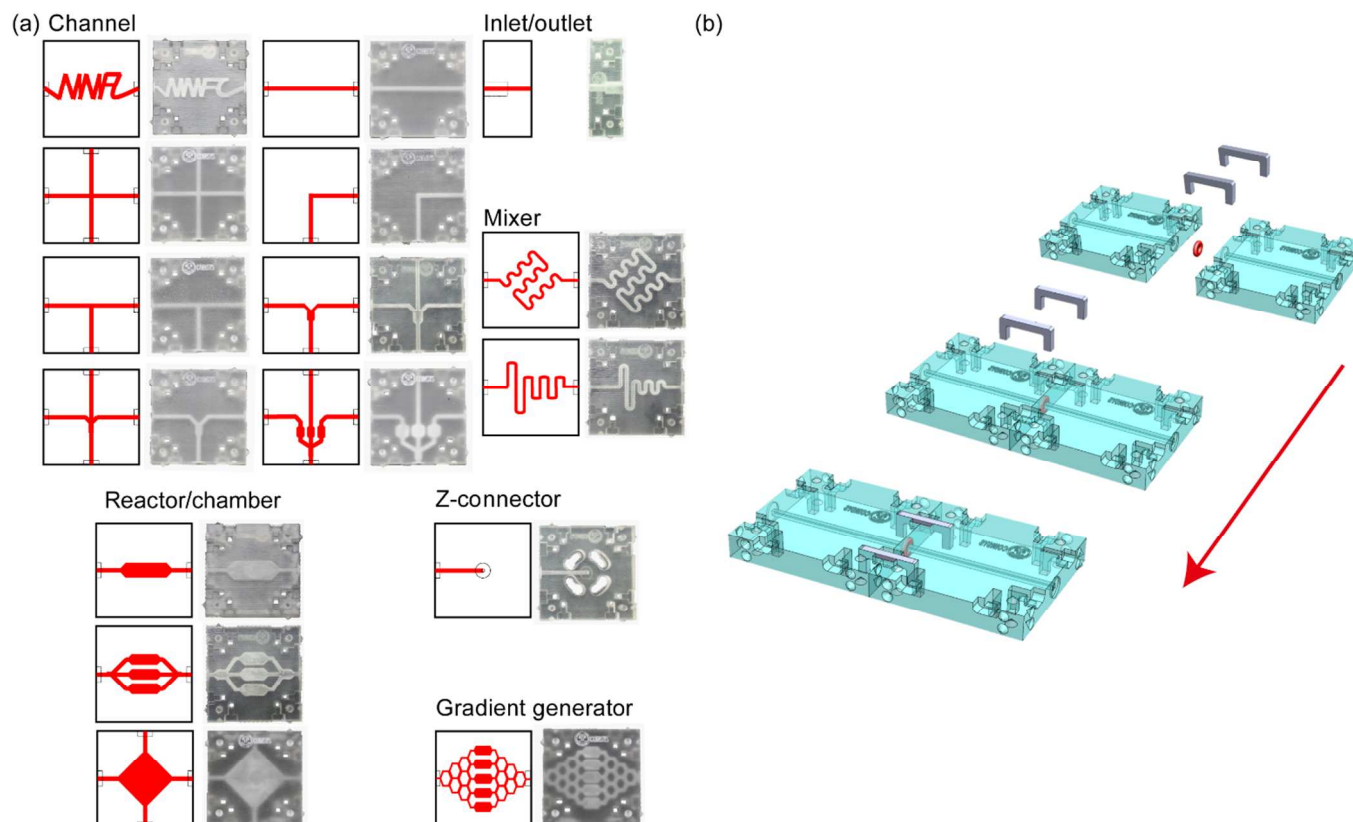


Fig. 1 (a) Schematic illustration and photographic images of functional modules (b) Schematic illustration of block chip assembly.

for inserting rubber O-rings. All the unique design features were illustrated in Fig. 1 and Fig. 2.

### Module Fabrication

The modules were directly printed from computer design using 3D printer. The module design for the customized microfluidic component was laid out in 3D using computer aided design (CAD) program for preparing geometric coordinates. From these data, the printer program automatically recognized multiple layered blueprints. Based on the coordinates, the print head precisely printed multiple layers of UV curable liquid polymer onto a flat surface. Once the polymers spread, UV lamp solidified the liquid polymers into hard polymers. During the process, wax also printed to fill out the void for preventing potential collapse of main structures. These processes were sequentially and repeatedly performed. After finishing all the processes, the wax was carefully removed from the microfluidic modules and the void became microchannels. These detailed processes were illustrated in Fig. S1. Direct printing of desired design into the working modules is

important. However, the limitation in printing resolution is inevitable due to the accuracy and size of printer components and rheological properties of raw material. To check the operating range of 3D printer, the microchannels were designed in the range of 100 ~ 1000  $\mu\text{m}$  in width and 50 ~ 500  $\mu\text{m}$  in height. From the obtained data, we compared dimensions of width and height of channels from design and actual modules as shown in Fig. S2 and Table S2. From given ranges, less than 100  $\mu\text{m}$  width and 50  $\mu\text{m}$  height of channels showed collapsed structure and inaccurate dimensions which may not be suitable to use. However, the microchannel width exhibited about 35  $\mu\text{m}$  differences between schematic design and actual module in the range of 100 to 1000  $\mu\text{m}$ . In addition, the height differences between design and printed modules were less than 11  $\mu\text{m}$  from a given range of 50 up to 500  $\mu\text{m}$ . Based on the observation, 3D printer showed better accuracy in vertical (*i. e.* height) than horizontal (*i. e.* width). Furthermore, the roughness of module surface was also investigated using atomic force microscopy (AFM) as shown in Fig. S3. The surface exhibits a surface

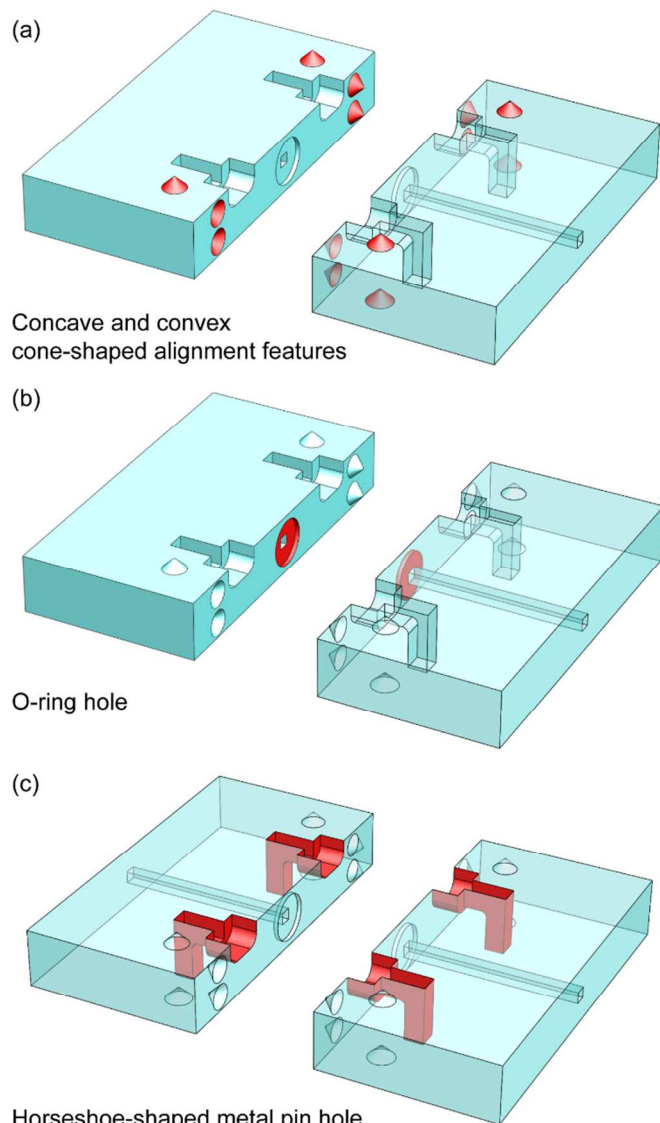


**Fig. 2** Unique design features for module assembly (a) cone-shaped alignment features, (b) o-ring hole, and (c) horseshoe-shaped metal pin hole.

roughness of 288 nm root mean square (RMS) for the module. All the dimension differences are similar to the given specification of 3D printer manufacturer. Therefore, the resolution of 3D printing indicated this method is suitable in the fabrication of module-based microfluidic devices.

### Assembly and connectivity

The sealing and connectivity are a significantly important in module-based system to prevent potential liquid leakage and device malfunction. In the macroscopic scale, the perfect connection without any solution losses may difficult due to the microscale inaccuracy at the interface of modules. Therefore, elastic material could be an alternative solution for perfect sealing because of its elasticity.<sup>14</sup> In this case, we inserted rubber O-ring between two modules as temporary sealing agent.

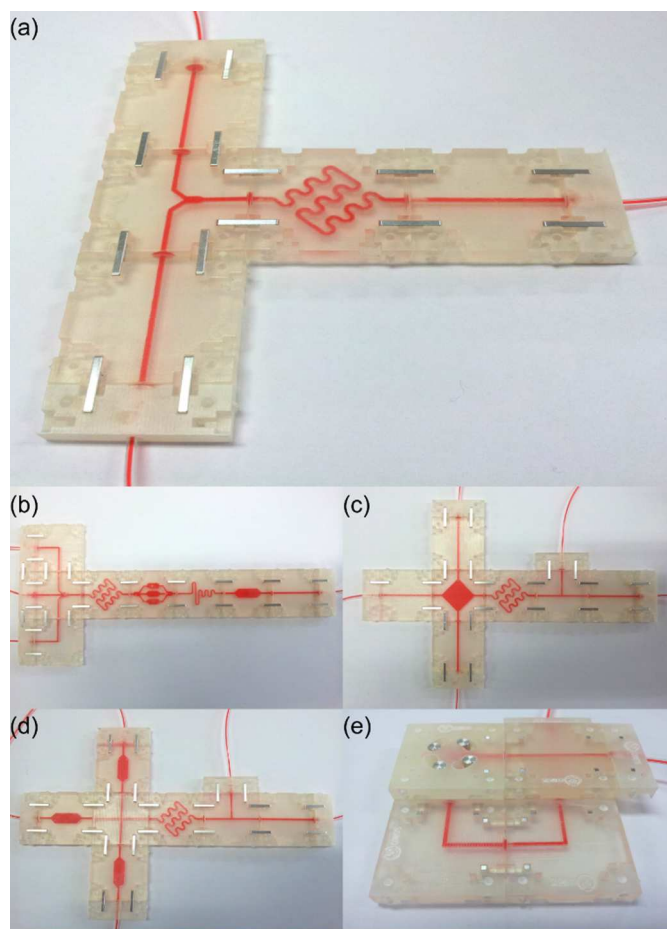


**Fig. 3** Photographic image of integrated microfluidic device for (a) biosensing and (b-e) several possible applications.

To check the capability of rubber cushion, we performed three different scenarios such as (a) without using O-ring, (b) pristine O-ring, and (c) O-ring with silicon grease. All modules were used digital pressure gauge and dye solution for leakage tests (Fig. S4a). The serious level of leakage of dyes solution was observed under no presence of O-ring connection (Fig. S4). On the contrast, the O-ring inserted modules can be held up to 200 kPa. Moreover, we also employed silicon grease around O-ring to upgrade its performance more than 800 kPa. As a result, the dramatic improvement in leakage resistance of O-ring (about 800 kPa) which is at least four times compared to pristine O-ring (200 kPa) as shown in Fig. S4c. These distinct phenomena mainly resulted from the hydrophobic nature of grease as barriers to minimize permeation of solution around interconnection area. As compared to previous reports, PDMS modules could maintain its functionality up to 40 kPa without using adhesive materials while PDMS sealed PDMS modules holding up to 200 kPa.<sup>13</sup> To address the recyclability of modules, potential different case of assembly and disassembly were also demonstrated in Fig. 3. The red ink flew in the channels for clear observation of different cases of assemblies. Overall, the main advantages of the modules are categorized into two parts. From the user's point of view, the modules easily convert into customized microfluidic device according to

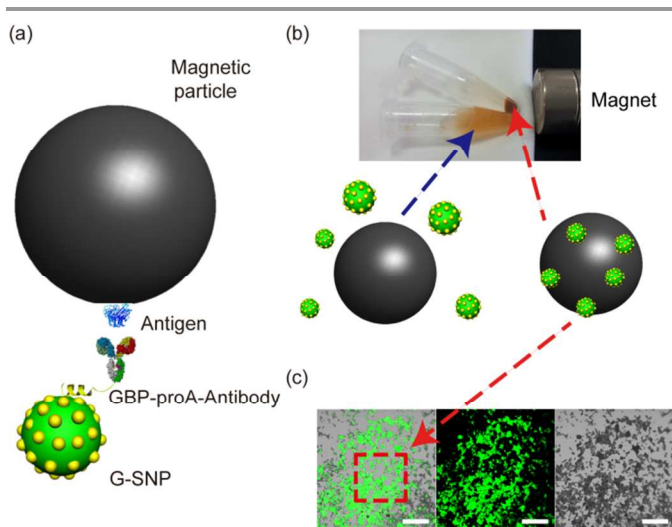


**Fig. 4** (a) Schematic illustration of specific binding of GFP-AFP fusion antigen on G-SNP and AFP antibody on magnetic particle. (b) Magnetic separation image of magnetic particles via specific antigen and antibody interaction and (c) its confocal fluorescent image. (Scale bar is 100  $\mu\text{m}$ )

users design. Note that the module assembly can be done anywhere without using any template and no glue is required. Comparing to other PDMS-based blocks,<sup>5,13</sup> these module-based components can be disassembled and re-assembled into functional microfluidic devices with O-ring and metal pins for different experimental purposes (Fig. 3). In addition, recycling of each module can save fabrication time and cost for further applications. Moreover, research community's perspective, the potential users who might benefit from the technology could adopt this system to spread the influence of microfluidics on their research.

#### Application of integrated device for cancer diagnosis

To demonstrate potential application of integrated devices as biosensor, we applied AFP immuno-reaction as an example for liver cancer diagnosis.<sup>15</sup> In this case, straight channels, Y-shaped channel, and mixer modules were selected to provide integrated device (Fig. 3a). The G-SNPs and carboxylated magnetic particles were chosen as templates for binding of GBP-proA-AFP antibodies and AFP antigens, respectively. The immobilized GBP-proA-AFP antibodies on G-SNPs specifically bind to AFP antigens conjugated magnetic particles. The combined particles were separated under magnetic field due to the strong interactions between AFP antigen and anti-AFP antibody while non-specific binding was not (Fig. 4b). Furthermore, the G-SNPs and magnetic particles complexes showed strong green fluorescent signal as shown in Fig. 4c. The proper overlap of fluorescent and optical images represented strong antibody and antigen interaction (*i.e.*, red square in Fig. 4c). The magnetically separated antibody and antigen conjugated particles were also observed using SEM (Fig. S5).

#### Conclusions

A straight forward, rapid, user friendly and cost-effective fabrication of module-based microfluidic components were successfully prepared by 3D printer. The designs were directly printed into functional 3D modules. Different scenario of module assembly displayed their functionality and recyclability. The variety designs of modules were firmly connected using metal pins and rubber O-rings. The inserted O-ring perfectly sealed the interconnection between the modules more firmly and prevented any solution leakage. The simple and easy module assembly and reconstruction are suitable expand microfluidics to non-expert users. Furthermore, the integrated microfluidic device and nano-/micro-particles were also applied as biosensors to detect AFP antigen. From this perspective, these techniques can be widely applicable in microfluidic-related researches including biosensing, biomedical, and biochemical devices.

### Experimental section

#### Module Fabrication

Modules were designed by assisting of AutoCAD computer software (Fig. 1 and Table S1) and directly printed using 3D printer (ProJet HD 3500 Plus, 3D Systems, USA) and raw UV curable polymer (VisiJet M3 Crystal, 3D Systems, USA). The printer has minimum feature size about 30  $\mu\text{m}$ . During the printing, all the inner microchannels were occupied of wax supports to prevent potential structural collapse. All the waxes were carefully removed from modules through sonication in ethanol bath and ready for assembly.

#### Module assembly

To assemble each module into a customized and integrated microfluidic device, the modules were aligned with each other and insert rubber O-ring between the channels. The modules were secured using metal pins at each corner. Unlike other methods, no surface treatment or substrates are required for assembly<sup>5,13</sup>.

#### Leakage test

The leakage test was manually performed under three different cases as following: (1) without rubber O-ring, (2) with rubber O-ring and (3) with greased rubber O-ring. Each pressure changes were measured more than 10 times using digital pressure gauge (PSB-1CP, Autonics, Korea) and dye solution.

#### Detection of AFP biomarker

The immuno-reaction was carried out using gold-deposited FITC-silica nanoparticles (G-SNPs) and carboxylated magnetic particles (Invitrogen, Life Technologies). As prepared 1 mL of G-SNPs (1 mg/mL) and 1 mL of gold binding protein-protein A fusion protein (GBP-proA, 200  $\mu\text{g}/\text{mL}$ ) were mixed for an hour at 25  $^{\circ}\text{C}$ . After GBP-proA immobilization on the surface of G-SNPs, the complexes were washed thoroughly to remove unbound proteins. For further immobilization of anti-AFP antibody, 100  $\mu\text{L}$  of the anti-AFP antibody (100  $\mu\text{g}/\text{mL}$ )

were added to the GBP–proA fusion protein immobilized G–SNPs solution for an hour. Conjugation of AFP antigen to magnetic particles were conducted using 100  $\mu$ L of AFP antigen (400  $\mu$ g/mL), 200  $\mu$ L of ethyl(dimethylaminopropyl) carbodiimide (EDC), and *N*-hydroxysuccinimide (NHS) with 500  $\mu$ L of magnetic particles (100  $\mu$ g/mL). After washing, bovine serum albumin (BSA) also used to prevent non-specific binding of anti–AFP antibody. Subsequently, anti–AFP antibody immobilized G–SNPs and AFP antigen conjugated magnetic particles solution were separately injected to integrated microfluidic device (Fig. 3a) to demonstrate the biosensing application. The immuno–reaction was observed by confocal microscopy (Carl Zeiss LSM 510 Meta, Germany) and Field–emission Scanning Electron Microscope (FE–SEM, S–4800, Hitachi).

### Acknowledgements

This work was supported by BioNano Health–Guard Research Center funded by the Ministry of Science, ICT & Future Planning (MSIP) of Korea as Global Frontier Project (Grant Number H–GUARD\_2013M3A6B2078945), by the Public Welfare & Safety Research Program through the National Research Foundation of Korea (NRF) funded by the MSIP of Korea (NRF–2013M3A2A1073991). It was also funded from the National Fisheries Research & Development Institute (NFRDI; contribution number RP–2013–BT–XXX).

### Notes and references

<sup>a</sup> Center for Nanobio Integration & Convergence Engineering (NICE), National Nanofab Center, 291 Daehak-ro, Yuseong-gu, Daejeon 305-806, Republic of Korea; E-mail: sjlee@nnfc.re.kr, tjlee@nnfc.re.kr

<sup>b</sup> Department of Chemical & Biomolecular Engineering, KAIST, 291 Daehak-ro, Yuseong-gu, Daejeon 305-701, Republic of Korea

<sup>c</sup> National Fisheries Research and Development Institute, 216 Haean-ro, Gijang-up, Gijang-gun, Busan 619-705, Republic of Korea

<sup>d</sup> Biomedical Engineering, School of Medicine, Keimyung University, 1095 Dalgubeol-daero, Dalseo-gu, Daegu 704-701, Republic of Korea

† Footnotes should appear here. These might include comments relevant to but not central to the matter under discussion, limited experimental and spectral data, and crystallographic data.

Electronic Supplementary Information (ESI) available: [Scheme and photographic images of modules, integrated device for biosensing application, unique mechanical alignment features, 3D printing mechanism, module assembly scenarios, SEM images of magnetic-silica complex, detailed dimension of module components, and comparison of 3D printing microchannel designed and measured dimension were demonstrated]. See DOI: 10.1039/c000000x/

- 1 D. Mark, S. Haeberle, G. Roth, F. Stetten and R. Zengerle, *Chem. Soc. Rev.*, 2010, **39**, 1153-1182.
- 2 A. B. Theberge, F. Courtois, Y. Schaerli, M. Fischlechner, C. Abell, F. Hollfelder, and W. T. S. Huck, *Angew. Chem. Int. Ed.*, 2010, **49**, 5846-5868.
- 3 C. D. Chin, V. Linder and S. K. Sia, *Lab Chip*, 2012, **12**, 2118-2134.

- 4 B. Kintsjes, L. D. van Vliet, S. R. A. Devenish, and F. Hollfelder, *Curr. Opin. Chem. Biol.*, 2010, **14**, 548-555.
- 5 S. M. Langelier, E. Livak-Dahl, A. J. Manzo, B. N. Johnson, N. G. Walter and M. A. Burns, *Lab Chip*, 2011, **11**, 1679-1687.
- 6 E. Bassoli, A. Gatto, L. Iuliano and M. G. Violante, *Rapid Prototyping Journal*, 2007, **13**, 148-155.
- 7 M. D. Symes, P. J. Kitson, J. Yan, C. J. Richmond, G. J. T. Cooper, R. W. Bowman, T. Vilbrandt and L. Cronin, *Nat. Chem.*, 2012, **4**, 349-354.
- 8 P. J. Kitson, M. H. Rosnes, V. Sans, V. Dragone and L. Cronin, *Lab Chip*, 2012, **12**, 3267-3271.
- 9 D. B. Kolesky, R. L. Truby, A. Sydney Gladman, T. A. Busbee, K. A. Homan and J. A. Lewis, *Adv. Mater.*, 2014, **26**, 3124-3130.
- 10 V. Mironov, T. Boland, T. Trusk, G. Forgacs and R. R. Markwald, *Trends Biotechnol.*, 2003, **21**, 157-161.
- 11 K. B. Anderson, S. Y. Lockwood, R. S. Martin and D. M. Spence, *Anal. Chem.*, 2013, **85**, 5622-5626.
- 12 A. K. Au, W. Lee and A. Folch, *Lab Chip*, 2014, **14**, 1294-1301.
- 13 M. Rhee and M. A. Burns, *Lab Chip*, 2008, **8**, 1365-1373.
- 14 O. H. Paydar, C. N. Paredes, Y. Hwang, J. Paz, N. B. Shah and R. N. Candler, *Sens. Actuators, A*, 2014, **205**, 199-203.
- 15 K. G. Lee, R. Wi, T. J. Park, S. H. Yoon, J. Lee, S. J. Lee and D. H. Kim, *Chem. Commun.*, 2010, **46**, 6374-6376.